Influence of structural isomerism and fluorine atom substitution on the self-association of naphthoic acid

Article (Accepted Version)

Influence of Structural Isomerism and Fluorine Atom Substitution on the Self-Association of Naphthoic Acid

*Roseanne Briffitt and Iain J. Day**

School of Life Sciences, University of Sussex, Falmer, Brighton, BN1 9QJ, UK

** To whom correspondence should be addressed:*

Telephone: +44 01273 876622

Fax: +44 01273 876687

Email: i.j.day@sussex.ac.uk

Keywords: Self-association, NMR, Chemical Shift, Equilibrium

Abstract

The self-association of small aromatic systems driven by π-π stacking and hydrophobic interactions is well known. Understanding the nature of these interactions is important if they are to be used to control association. Here, we present results of an NMR study into the self-association of two isomers of naphthoic acid along with an investigation into the role of a fluorine substituent on that self-association. We interpret the results in terms of a simple isodesmic model of self-association and show that the addition of the fluorine atom appears to increase the stability of the aggregates by an order of magnitude (e.g. 1-naphothic acid vs 4-fluoro-1-naphthoic acid K_{eq} = 0.05 increases to 0.35 M^{-1}), a result which is supported by computational studies in the literature on the role of substituent effects on interaction energy. The use of fluorinated isomers to probe the assembly is also presented, with differing trends in fluorine-19 chemical shifts observed depending on the isomer substitution pattern.

Introduction

Small aromatic molecules often undergo self-assembly in aqueous solution, driven by non-covalent interactions such as π-π stacking and the hydrophobic effect.[1,2] These interactions can result in dramatic changes to physicochemical properties, such as light absorption[3] or solubility, and hence self-assembly phenomena have been the subject of much investigation, in areas as diverse as the impact on drug solubility and solvent partitioning,[4] the intercalation of small molecules into DNA[5-8] and the propensity of some systems to form liquid crystals at high concentrations.[9-13] Typically, small molecule self-association is observed in aromatic systems where π-π stacking interactions are important,[14-16] or in amphipathic systems leading to micelle or other large assembly formation.[17] Multicomponent systems are also important, probing the role of functional groups in aggregation[18-20] and drug delivery.[21-24]

A number of physical techniques can provide information on aggregation processes such as optical absorption,[3] x-ray scattering[3,13,25,26] and nuclear magnetic resonance (NMR) spectroscopy.[10,12,26-28] In general, absorption and scattering based experiments provide information on the bulk properties of a sample, e.g. average aggregate sizes etc. NMR spectroscopy is almost unique in the fact that it can give information at an atomic level of detail, albeit averaged over the ensemble of molecules present in the sample. Previously we have utilised NMR spectroscopy to investigate the self-aggregation of the azo-dye sunset yellow as a function of concentration.[28] This well-studied system[3,10-13,25] provided an ideal demonstration of the utility of NMR spectroscopy for the investigation of aromatic self-aggregation. More recently, we have explored the interaction of a structurally similar small probe molecule with sunset yellow. In these studies two different motifs were used: fluorophenols[27] and an

isomer of fluoronaphthoic acid,[29] both of which were chosen so as to mimic part of the sunset yellow structure. The inclusion of the fluorine atom provided a unique NMR-active reporter nucleus with which to track the interaction of the small molecule with the sunset yellow assemblies. As part of these studies, the self-association properties of the small probe molecules themselves (i.e. in the absence of sunset yellow) were briefly investigated. While the various fluorophenols did not show any evidence of aggregation at the concentrations investigated,[27] the same was not true of 6-fluoro-2-naphthoic acid, which showed some weak self-association.[29]

In this article we explore in more detail the self-association of some naphthoic acids, including the effects of structural isomerism (1- vs 2-naphthoic acid) and the influence of introducing a fluorine atom into the structure. The structures and abbreviations of the compounds used in this work are given in Figure 1. We use a combination of NMR methods, namely changes in chemical shifts and diffusion coefficients, similar to those reported previously[27,29] and interpret the results in terms of the simple isodesmic model of self-association.[27,29,30]

Materials and Methods

Materials

Deuterium oxide was purchased from Goss Scientific (Cheshire, UK). All other chemicals were purchased from Sigma Aldrich (Dorset, UK) and used as obtained. Stock solutions of each of the naphthoic acids were prepared at a concentration of 150 mM, or 90 mM in the case of 6-fluoro-2-naphthoic acid, in deuterium oxide. In order to improve the aqueous solubility 1.1 equivalents of sodium deuteroxide were added to produce the corresponding sodium naphthoate salt. It was noted that after

prolonged storage the fluoronaphthoates underwent defluorination via an S_NAr type reaction.[31] In order to mitigate against this, the stock solutions of the fluoronaphthoates were lyophilised (Genevac EZ-2, Ipswich, UK) and stored at -20 °C until required. The stock solutions were diluted with deuterium oxide to achieve the desired concentrations.

NMR Spectroscopy

All NMR data were collected on a Varian VNMRS 600 spectrometer (Agilent Technologies, Yarnton, UK) using an X{^{1}H-^{19}F} probe equipped with a *z*-axis gradient capable of producing 0.7 T m^{-1}. The sample temperature was maintained at 298 K throughout the experiments.

^{1}H-detected diffusion NMR experiments were performed using the Oneshot sequence[32] with a diffusion labelling period of 100 ms, and 15 diffusion encoding gradients, each of 2 ms duration, with intensities between 0.0202 and 0.6066 T m^{-1} equally spaced in g^2. The data were processed using the DOSY Toolbox[33] with the appropriately modified Stejskal-Tanner equation for the Oneshot sequence.[32]

Data Analysis

The isodesmic model of self-association was used to obtain equilibrium constants from the concentration dependent chemical shifts.[27,29] This model has been extensively reviewed by Martin[30] and only the salient points will be reproduced here. The main assumptions behind this model are that the addition of each monomer to a growing assembly occurs with the same, equal, equilibrium constant, i.e. $K_1 = K_2 = \ldots = K_n = K_{eq}$, and that the observed chemical shift can be described by the weighted

sum of the chemical shifts of the free monomers and molecules within the assemblies. End effects are accounted for by the assumption that molecules at the end of a stack experience half the additional shielding contribution of molecules within the stack. These assumptions allow the observed chemical shift δ_{obs} to be written as:[30]

$$\delta_{obs} = \delta_{mon} + (\delta_{int} - \delta_{mon}) \frac{2K_{eq}c_T + 1 - \sqrt{4K_{eq}c_T + 1}}{2K_{eq}c_T} \quad (1)$$

where δ_{mon} and δ_{int} are the chemical shifts of the free monomer and a molecule in the interior of the stack respectively and c_T is the total sample concentration.

The isodesmic model can be extended to account for the interaction of a second species, present at low concentration, with the aggregate assemblies.[29,30] The observed chemical shift for the second species in the fast exchange limit is given as the weighted average of the chemical shifts of the unbound monomer, end-binders and internally inserted second molecules:

$$\delta^B_{obs} = a\delta^B_{mon} + b\delta^B_{end} + c\delta^B_{int} \quad (2)$$

where the appropriate mole fractions are given as:

$$a = \frac{1}{1 + K_1[A_e] + K_1K_2[A_e]^2} \quad (3)$$

$$b = \frac{K_1[A_e]}{1 + K_1[A_e] + K_1K_2[A_e]^2}$$

$$c = \frac{K_1K_2[A_e]^2}{1 + K_1[A_e] + K_1K_2[A_e]^2}$$

and $[A_e]$ is the concentration of the aggregate ends, which can be calculated using:

$$[A_e] = 2c_T\left(1 - \alpha K_{eq}c_T\right) \quad (4)$$

with K_{eq} being the equilibrium constant for the association of the major species at concentration c_T with α stack ends.[27,29,30]

Data analysis was performed by implementing the models described above using the open source SciPy library[34] of the Python programming language. Error estimation in the fitted parameters was performed using Monte Carlo methods.[35]

Results and Discussion

Simple single component self-association

Initial investigations into the self-association of naphthoic acid were performed using the two structural isomers, 1-naphthoic acid (1NA) and 2-naphthoic acid (2NA) shown in Figure 1. In order to improve the aqueous solubility, the corresponding sodium naphthoate salts were produced by the addition of sodium deuteroxide to the stock solutions. Unless otherwise noted, the sodium napthoate salts were used throughout this work. The ^{1}H chemical shifts of the aromatic resonances in 1NA and 2NA were followed as a function of concentration. Example ^{1}H NMR spectra of 1NA are shown in Figure 2(a) with the chemical shifts plotted as a function of concentration for 1NA in Figure 2(b) and 2NA in Figure 2(c). Due to the extensive overlap in parts of the spectrum, regions of interest are followed, rather than specific signals. Both species show evidence of weak self-association as indicated by the decrease in observed chemical shift with increasing concentration, with this effect being more pronounced for 2NA, being of the order of $\Delta\delta$ = -0.15 ppm, compared to $\Delta\delta$ = -0.04 ppm for 1NA. This decrease in chemical shift is attributed to an increase in shielding caused by π-π overlap when the molecules come into close proximity.[1,30] Application of the isodesmic model[30] as given in eq 1 to these data resulted in the equilibrium constants quoted in Table 1, with the value for 1NA being around twice that for 2NA. The position of the carboxylate group therefore appears to have a minor effect on the weak self-association of naphthoic acid. Naphthalene itself forms a

herringbone like arrangement with a combination of face-face and face-end π-π stacking.[36] Addition of the carboxyl group opens up the possibility of hydrogen bonding as a major factor in determining the nature of the interaction between molecules. The position of the carboxyl group is clearly important, for example, in the solid state different stacking arrangements of 1NA and 2NA have been reported.[37] In both molecules, cyclic dimers are formed between carboxylic acid groups, with a slipped stacking motif in the case of 1NA putting the carboxyl carbon over a carboxyl oxygen of a lower layer. In the case of 2NA, the stacking is slightly different, putting the carboxyl carbon over the *meta*-carbon in the lower layer.[37] While these arrangements are not likely to hold directly in solution, the positioning of one layer over the other in a staggered manner is consistent with the observed changes in ^{1}H chemical shifts arising from π-π stacking.[1]

Our previous investigations into self-association phenomena have utilised fluoronaphthoic acids[29] hence the effect on the self-association of including the fluorine atom in the naphthoic acid structure is of interest. Similar experiments were performed with two readily available fluorinated isomers: 4-fluoro-1-naphthoic acid (4F1NA) and 6-fluoro-2-napththoic acid (6F2NA), monitoring both the ^{1}H and ^{19}F chemical shifts. Sample ^{1}H and ^{19}F spectra for 6F2NA are shown in Figure 3(a) and 3(b), while the plots of the respective chemical shifts as a function of concentration are in Figures 3(c)-(f) for both isomers. Fitting just the ^{1}H chemical shifts (Figures 3(c) and (d)) to the isodesmic model gives the equilibrium constants presented in Table 1. These equilibrium constants are larger than those for 1NA and 2NA, indicating that there is a greater degree of self-association occurring upon inclusion of the fluorine substituent into the naphthoate structure. Since the ^{19}F chemical shift of

the fluorine substituent was also monitored (Figures 3(e) and (f)), including this data into the fitting procedure results in a slight modification to the measured equilibrium constants, these are also given in Table 1. While the equilibrium constant for 6F2NA is relatively unchanged, there is a dramatic change for 4F1NA of around 0.3 M^{-1}. As can be seen from Figure 3(c), the change in ^{1}H chemical shift with increasing naphthoate concentration is rather shallow, although there is a change of around -0.02 to -0.06 ppm over the concentration range used. This means that the possibility of extracting a reliable equilibrium constant by the fitting of eq 1 to these data is limited. Inclusion of the ^{19}F chemical shift data in the fitting procedure adds an additional constraint to the fitted parameters and hence allows a more reliable value for K_{eq} to be obtained. The inclusion of the ^{19}F data in the case of 6F2NA does not yield significant improvement as the ^{1}H chemical shifts all show greater concentration dependence than in the case of 4F1NA. As can been seen by the equilibrium constants given in Table 1, the incorporation of the fluorine substituent into the naphthoate structure has a significant impact on the self-association. While the overall self-association is still relatively weak, the equilibrium constant is increased by almost an order of magnitude upon inclusion of the fluorine. The position of the fluorine, and its relationship to the position of the carboxylic acid group, does also have a small role in the degree of self-association. In this case, 4F1NA shows a slightly greater tendency to self-associate than 6F2NA under these conditions, in line with that observed for the parent nathphoic acids.

^{1}H-detected diffusion NMR measurements were also recorded to monitor changes in the overall average size of the species as a function of concentration in solution, with these data being shown in Figure 4. Whilst there is a notable degree of error in the

measurements, particularly at the very low, sub-millimolar, concentrations due to low signal-to-noise presented by these samples, there is a clear decrease in the observed diffusion coefficient for each naphthoic acid isomer with increasing sample concentration. This trend in decreasing diffusion coefficient is consistent with the formation of larger assemblies at higher concentration and is similar to trends seen with other self-associating aromatic systems, such as sunset yellow.[27-29] While it is possible that there is an increase in solvent viscosity with increasing naphthoic acid concentration this is unlikely to be responsible for the observed changes in chemical shift. Any change in sample viscosity would typically result in a change in the spectral line width.[38] The reason for this is that as molecular tumbling becomes slower, transverse relaxation would become more efficient, resulting in broader signals.[38] This effect has been seen in previous work on sunset yellow; peaks broaden due to increases in sample viscosity, but change in chemical shift as a result of self-association.[10,12,28,39]

It is not clear exactly what structural features are ultimately responsible for the differences in interactions between the various nathphoic acid isomers. It is known that differences in dipole and quadrupole moments can be responsible for the strong association of benzene and hexafluorobenzene.[40,41] The dipole moments for the naphthoic acid isomers are presented in Table 2. The position of the carboxylic acid group has little effect on the dipole moment, while addition of the fluorine substituent, typically opposite the carboxylic acid, reduces the overall polarity of the naphthoic acid. While the two fluorinated isomers are similar, 6F2NA has the smallest dipole moment, being around one quarter that of the parent naphthoic acids.

Using fluoronaphthoic acid as a probe of naphthoic acid association

Our previous NMR investigations of small molecule self-assembly have utilised the azo dye sunset yellow[28] and more recently, focused on the interaction of small, structurally similar probe molecules with the larger assemblies.[27,29] These small probe molecules contained a fluorine substituent to be used as an NMR reporter. Using the naphthoate system described here it is possible to investigate the effect of including the fluorine substituent by adding a small amount of one of the fluorinated isomers at low concentration (typically around 1 mol%) to the solution of the relevant naphthoic acid, i.e. 1NA plus 1 mol% 4F1NA. ^{1}H chemical shifts of the major naphthoic acid component were followed as a function of sample concentration in the presence of 1 mol% of a fluorinated naphthoic acid. The results for all four possible combinations are shown in Figure 5. Comparable changes in the observed chemical shifts as a function of concentration to those in the case of pure naphthoic acid samples were observed. The changes were of the order of -0.01 to -0.04 ppm and -0.08 to -0.60 ppm for the 1NA and 2NA samples respectively. Fitting these data to the isodesmic model presented in eq 1 yields the equilibrium constants given in Table 3. There is little difference in the fitted equilibrium constant in the case of 1NA with either of the fluorinated isomers, while in the case of 2NA there is a notable increase in the equilibrium constant, especially in the case of 1 mol% 6F2NA where the equilibrium constant increases by an order of magnitude. This indicates that the addition of 1 mol% 6F2NA to the solution of 2NA causes a marked increase in the stability of the assemblies formed. This is in contrast to the situation when 1mol% 6F2NA was added to solutions of sunset yellow, where a decrease in the sunset yellow self-association equilibrium constant of around 30% was noted.[27,29]

The inclusion of the fluorine nucleus on the second molecule allowed the ^{19}F chemical shift to be followed as a function of naphthoic acid concentration, and act as a reporter of the interaction between the fluoronaphthoic acid and the non-fluorinated main component. The results of these measurements are shown in Figure 6. A number of different trends are observed, depending on whether 4F1NA or 6F2NA is present at 1 mol%. In the case of 4F1NA being added, there is a general increase in the observed ^{19}F chemical shift with increasing naphthoic acid concentration. This is similar for both structural isomers, however, 2NA shows an additional feature of a slight minimum at a concentration of around 40 mM, similar to that seen in the interaction of the isomers of fluorophenol with sunset yellow.[27] This general trend of an increase in ^{19}F chemical shift indicates that the fluorine nucleus is experiencing a decrease in shielding. This is in contrast to the trend usually observed for π-π stacking in which an increase in shielding is seen due to overlap of the π orbitals.[1] The situation is noticeably different using 6F2NA present at 1 mol% with either of the naphthoic isomers. In this case, the observed ^{19}F chemical shift generally decreases with increasing naphthoic acid concentration. In the case of 1NA being the major component, although there is a reasonable amount of scatter in the data, there is a trend which is the opposite of that observed in the 2NA + 4F1NA system, in that there is an initial increase in ^{19}F chemical shift up to 40 mM naphthoic acid, then a subsequent decrease with increasing sample concentration. In the case of 6F2NA at 1 mol% in 2NA there is a monotonic decrease in the ^{19}F chemical shift with increasing naphthoic acid concentration. The solid lines in Figure 6 show a fit to the isodesmic model, extended to include the interaction of a second species present at low concentration.[27,29,30] This model comprises two equilibrium constants, for interaction of the second species at the end or interior of the aggregate assemblies,[30] with the

corresponding parameters obtained from fitting eq 2 to the ^{19}F chemical shift data given in Table 4. With the exception of the 1NA + 4F1NA system, the equilibrium constants suggest that the predominant binding mode is insertion into the aggregated stacks of naphthoic acid, with K_2 being larger than K_1 in all cases. While the errors are large for these parameters, they do suggest that there is an appreciable interaction between the naphthoic acid and the fluorinated isomer. This is in line with the increased aggregate stability noted from the analysis of the ^{1}H chemical shifts.

Conclusions

The association of small aromatic molecules in aqueous solution, driven by π-π stacking interactions is well known.[1,2,42] Understanding the factors which affect these assembly processes is an active field of research. Here, we have investigated the weak self-association of two isomers of naphthoic acid and some monofluorinated variants. Using NMR spectroscopy, we have demonstrated that the inclusion of a fluorine substituent increases the stability of the aggregates formed, by an order of magnitude (K_{eq} = 0.2-0.3 M^{-1} vs 0.02-0.05 M^{-1}) and by tracking ^{19}F chemical shifts in mixed systems that the major binding mode is generally insertion into the aggregates rather than binding at the ends of the stacks. There are distinct differences in the trends of ^{19}F chemical shift for 4F1NA vs 6F2NA with decreased shielding observed for the former, but an increase in shielding for the latter. The substitution pattern of the functional groups around the naphthalene core plays a role in this increased stability, with 1mol% 6F2NA providing a greater degree of stabilisation than 4F1NA to the assemblies of naphthoic acids by an order of magnitude. The increase in stability upon addition of fluoronaphthoic acid is similar to effects which have been reported utilising high level calculations to determine the binding energies of various pairs of

substituted benzenes.[43] The addition of a fluorine atom increased the interaction energy by 0.6 kcal mol^{-1} and decreased the binding distance by 0.1 Å.[43] More recently, further calculations have shown that substituent effects on aromatic stacking interactions are influenced both by changes in the π-density and in the polarity of the substituent bond, with the latter usually being the major contributor.[44] Indeed, it has long been known that intermolecular π-π interactions, crystal packing effects and liquid crystal behaviour can be controlled by tuning fluoroaromatic interactions.[40,41,45]

Acknowledgements

The authors thank Jonathan Katz and Prof. Mark Bagley for helpful discussions and Michael Paradowski for assistance with the lyophiliser. The University of Sussex is acknowledged for financial support.

References

(1) Hunter, C. A.; Sanders, J. K. M. The Nature of pi-pi Interactions. *J. Am. Chem. Soc.* **1990**, *112*, 5525-5534.

(2) Martinez, C. R.; Iverson, B. L. Rethinking the Term "pi-Stacking". *Chem. Sci.* **2012**, *3*, 2191-2201.

(3) Horowitz, V. R.; Janowitz, L. A.; Modie, A. L.; Heiney, P. A.; Collings, P. J. Aggregation Behaviour and Chromonic Liquid Crystal Properties of an Anionic Monoazo Dye. *Phys. Rev. E* **2005**, *72*, 041710.

(4) Lock, L. L.; Lacomb, M.; Schwarz, K.; Cheetham, A. G.; Lin, Y.-A.; Zhang, P.; Cui, H. Self-Assembly of Natural and Synthetic Drug Amphiphiles into Discrete Supramolecular Nanostructures. *Faraday Discuss.* **2013**, *166*, 285-301.

(5) Dougherty, G.; Pilbrow, J. R. Physico-Chemical Probes of Intercalation. *Int. J. Biochem.* **1984**, *16*, 1179-1192.

(6) Rescifina, A.; Zagi, C.; Varrica, M. G.; Pistara, V.; Corsaro, A. Recent Advances in Small Organic Molecules as DNA Intercalating Agents: Synthesis, Activity and Modelling. *Eur. J. Med. Chem.* **2014**, *74*, 95-115.

(7) Singh, S. K.; Pandey, D. S. Multifaceted Half-Sandwich Arene-Ruthenium Complexes: Interactions with Biomolecules, Photoactivation and Multinuclearity Approach. *RSC Advances* **2014**, *4*.

(8) Sirajudin, M.; Ali, S.; Badshah, A. Drug-DNA Interactions and Their Study by Uv-Visible, Fluorescence Spectroscopies and Cyclic Voltametry. *J. Photochem. Photobiol. B* **2014**, *124*, 1-19.

(9) Lydon, J. Chromonic Mesophases. *Curr. Opin. Colloid. In. Sci.* **2004**, *8*, 480-490.

(10) Edwards, D. J.; Jones, J. W.; Lozman, O.; Ormerod, A. P.; Sintyureva, M.; Tiddy, G. J. T. Chromonic Liquid Crystal Formation by Edicol Sunset Yellow. *J. Phys. Chem. B* **2008**, *112*, 14628-14636.

(11) Park, H.-S.; Kang, S.-W.; Tortora, L.; Nastishin, Y.; Finotello, D.; Kumar, S.; Lavrentovich, O. D. Self-Assembly of Lyotropic Chromonic Liquid Crystal Sunset Yellow and Effects of Ionic Additives. *J. Phys. Chem. B* **2008**, *112*, 16307-16319.

(12) Jones, J. W.; Lue, L.; Ormerod, A. P.; Tiddy, G. J. T. The Influence of Sodium Chloride on the Self-Association and Chromonic Mesophase Formation of Edicol Sunset Yellow. *Liq. Cryst.* **2010**, *37*, 711-722.

(13) Park, H.-S.; Kang, S.-W.; Tortora, L.; Kumar, R.; Lavrentovich, O. D. Condensation of Self-Assembled Lyotropic Chromonic Liquid Crystal Sunset Yellow

in Aqueous Solutions Crowded with Polyethylene Glycol and Doped with Salt. *Langmuir* **2011**, *27*, 4164-4175.

(14) Davies, D. B.; Djimant, L. N.; Veselkov, A. N. 1H NMR Investigation of Self-Association of Aromatic Drug Molecules in Aqueous Solution. *J. Chem. Soc. Faraday Trans.* **1996**, *92*, 383-390.

(15) Zeng, P.; Zhang, G.; Rao, A.; Bowles, W.; Wiedmann, T. S. Concentration Dependent Aggregation Properties of Chlorhexidine Salts. *Int. J. Pharm.* **2009**, *367*, 73-78.

(16) Shetty, A. S.; Zhang, J.; Moore, J. S. Aromatic pi-Stacking in Solution as Revealed through the Aggregation of Phenylacetylenen Macrocycles. *J. Am. Chem. Soc.* **1996**, *118*, 1019-1027.

(17) Abbandonato, G.; Catalano, D.; Marini, A. Aggregation of Perfluoroctanoate Salt Studied by 19f NMR and DFT Calculations: Counterion Complexation, Poly(Ethylene Glycol) Addition and Conformational Effects. *Langmuir* **2010**, *26*, 16762-16770.

(18) Aradi, F. Comparative 1H NMR Chemical Shift Study on the Stacking Interaction of Pyrimidine with Purine and 6-Methylpurine. *Biophys. Chem.* **1992**, *44*, 143-150.

(19) Aradi, F. Effect of Methylation on the Pyrimidine-Pyrimidine Stacking Interaction Studied by 1H NMR Chemical Shift. *Biophys. Chem.* **1995**, *54*, 67-73.

(20) Dimicoli, J.-L.; Helene, C. Complex Formation between Purine and Indole Derivatives in Aqueous Solution. Proton Magnetic Resonance Studies. *J. Am. Chem. Soc.* **1973**, *95*, 1036-1044.

(21) Schreier, S.; P., M. S. V.; de Paula, E. Surface Active Drugs: Self-Association and Interaction with Membranes and Surfactants. Physicochemical and Biological Aspects. *Biochim. Biophys. Acta* **2000**, *1508*, 210-234.

(22) Srivastava, S.; Phadke, R. S.; Govil, G. Effect of Incorporation of Drugs, Vitamins and Peptides on the Structure and Dynamics of Lipid Assemblies. *Mol. Cell. Biochem.* **1989**, *91*, 99-109.

(23) Matsumori, N.; Tahara, K.; Yamamoto, H.; Morooka, A.; Doi, M.; Oishi, T.; Murata, M. Direct Interaction between Amphotericin B and Ergosterol in Lipid Bilayers as Revealed by 2H NMR Spectroscopy. *J. Am. Chem. Soc.* **2009**, *131*, 11855-11860.

(24) Da Costa, G.; Mouret, L.; Chevance, S.; Le Rumeur, E.; Bondon, A. NMR of Molecules Interacting with Lipids in Small Unilamellar Vesicles. *Eur. Biophys. J.* **2007**, *36*, 933-942.

(25) Joshi, L.; Kang, S.-W.; Agra-Kooijman, D. M.; Kumar, S. Concentration, Temperature, and pH Dependence of Sunset-Yellow Aggregates in Aqueous Solution: An x-ray Invesitgation. *Phys. Rev. E.* **2009**, *80*, 041703.

(26) Hutin, M.; Sprafke, J. K.; Odell, B.; Anderson, H. L.; Claridge, T. D. W. A Discrete Three-Layer Stack Aggregate of a Linear Porphyrin Tetramer: Solution Phase Structure Elucidation by NMR and x-ray Scattering. *J. Am. Chem. Soc.* **2013**, *135*, 12798-12807.

(27) Katz, J. R.; Day, L. J.; Day, I. J. NMR Investigations of the Interaction between the Azo-Dye Sunset Yellow and Fluorophenol. *J. Phys. Chem. B* **2013**, *117*, 11793-11800.

(28) Renshaw, M. P.; Day, I. J. NMR Characterization of the Aggregation State of the Azo Dye Sunset Yellow in the Isotropic Phase. *J. Phys. Chem. B* **2010**, *114*, 10032-10038.

(29) Katz, J. R.; Day, I. J. Investigating the Interaction of Sunset Yellow Aggregates and 6-Fluoro-2-Naphthoic Acid: Increasing Probe Molecule Complexity. *Magn. Reson. Chem.* **2014**, *52*, 435-439.

(30) Martin, R. B. Comparisons of Indefinite Self-Association Models. *Chem. Rev.* **1996**, *96*, 3043-3064.

(31) Carey, F. A.; Sundberg, R. J. *Advanced Organic Chemistry: Structure and Mechanism*; Plenum Press: New York, 1990.

(32) Pelta, M. D.; Morris, G. A.; Stchedroff, M. J.; Hammond, S. J. A One-Shot Sequence for High Resolution Diffusion-Ordered Spectroscopy. *Magn. Reson. Chem.* **2002**, *40*, S147-S152.

(33) Nilsson, M. The Dosy Toolbox: A New Tool for Processing PFG NMR Diffusion Data. *J. Magn. Reson.* **2009**, *200*, 296-302.

(34) Jones, E.; Oliphant, T.; Peterson, P. Scipy: Open Source Scientific Tools for Python, 2001.

(35) Press, W. H.; Flannery, B. P.; Teukolsky, S. A.; Vetterling, W. T. *Numerical Recipes in Fortran 77*; Cambridge University Press: Cambridge, 1992.

(36) Yavuz, I.; Martin, B. N.; Park, J.; Houk, K. N. Theoretical Studies of the Molecular Ordering, Paracrystallinity and Charge Mobilities of Oligomers in Different Crystaline Phases. *J. Am. Chem. Soc.* **2015**, *137*, 2856-2866.

(37) Fitzgerald, L. J.; Gerkin, R. E. Redetermination of the Structures of 1-Naphthoic Acid and 2-Naphthoic Acid. *Acta Cryst.* **1993**, *C49*, 1952-1958.

(38) Levitt, M. H. *Spin Dynamics*, Second ed.; John Wiley and Sons: Chichester, 2008.

(39) Tait, K. M.; Parkinson, J. A.; Gibson, D. I.; Richardson, P. R.; Ebenezer, W. J.; Hutchings, M. G.; Jones, A. C. Structural Characterisation of the Photoisomers of Reactive Sulfonated Azo Dyes by NMR Specctroscopy and DFT Calculations. *Photochem. Photobiol. Sci.* **2007**, *6*, 1010-1018.

(40) West Jr, A. P.; Mecozzi, S.; Dougherty, D. A. Theoretical Studies of the Supramolecular Synthon Benzene . . . Hexafluorobenzene. *J. Phys. Org. Chem.* **1997**, *10*, 347-350.

(41) Williams, J. H. The Molecular Electric Quadrupole Moment and Solid-State Architecture. *Acc. Chem. Res.* **1993**, *26*, 593-598.

(42) Sivadas, A. P.; Kumar, N. S. S.; Prabhu, D. D.; Varghese, S.; Prasad, S. K.; Rao, D. S. S.; Das, S. Supergelation Via Purely Aromatic pi-pi Driven Self-Assembly of Pseudodiscotic Oxadiazole Mesogens. *J. Am. Chem. Soc.* **2014**, *136*, 5416-5423.

(43) Sinnokrot, M. O.; Sherrill, C. D. Unexpected Substituent Effects in Face-to-Face pi-Stacking Interactions. *J. Phys. Chem. A* **2003**, *107*, 8377-8379.

(44) Parrish, R. M.; Sherrill, C. D. Quantum-Mechanical Evaluation of pi-pi Versus Substituent-pi Interactions in pi Stacking: Direct Evidence for the Wheeler-Houk Picture. *J. Am. Chem. Soc.* **2014**, *136*, 17386-17389.

(45) Dai, C.; Nguyen, P.; Marder, T. B.; Scott, A. J.; Clegg, W.; Viney, C. Control of Single Crystal Structure and Liquid Crystal Phase Behaviour Via Arene-Perfluoroarene Interactions. *Chem. Commun.* **1999**, 2493-2494.

(46) Hanwell, M. D.; Curtis, D. E.; Lonie, D. C.; Vandermeersch, T.; Zurek, E.; Hutchinson, G. R. Avogadro: An Advanced Semantic Chemical Editor, Visualization and Analysis Platform. *J. Cheminform.* **2012**, *4*, 17.

Tables and Table Captions

Table 1: Equilibrium constants obtained from fitting eq 1 to the data given in Figures 2 and 3.

Species	K_{eq} (M^{-1})	
	^{1}H chemical shifts only	Including ^{19}F chemical shifts
1NA	$(0.54 \pm 0.06) \times 10^{-1}$	n/a
2NA	$(0.21 \pm 0.06) \times 10^{-1}$	n/a
4F1NA	$(0.72 \pm 0.35) \times 10^{-1}$	$(3.51 \pm 1.25) \times 10^{-1}$
6F2NA	$(2.44 \pm 1.15) \times 10^{-1}$	$(2.45 \pm 1.14) \times 10^{-1}$

Table 2: Dipole moments for the various naphthic acids, calculated using Avogadro.[46]

Species	Dipole moment (D)
1NA	0.521
2NA	0.513
4F1NA	0.182
6F2NA	0.118

Table 3: Equilibrium constants obtained from fitting eq 1 to the data given in Figure 5.

Species + 1mol% probe	K_{eq} (M^{-1})

1NA + 4F1NA	$(0.50 \pm 3.11) \times 10^{-1}$
1NA + 6F2NA	$(0.52 \pm 2.17) \times 10^{-1}$
2NA + 4F1NA	$(0.37 \pm 0.22) \times 10^{-1}$
2NA + 6F2NA	$(2.51 \pm 1.10) \times 10^{-1}$

Table 4: Equilibrium constants obtained from fitting eq 2 to the data given in Figure 6.

Species + 1mol% probe	K_1 (M^{-1})	K_2 (M^{-1})
1NA + 4F1NA	$(5.74 \pm 7.45) \times 10^{3}$	$(2.18 \pm 3.25) \times 10^{-3}$
1NA + 6F2NA	$(0.51 \pm 9.50) \times 10^{1}$	$(7.25 \pm 30.2) \times 10^{1}$
2NA + 4F1NA	$(1.56 \pm 22.21) \times 10^{-1}$	$(4.50 \pm 5.75) \times 10^{2}$
2NA + 6F2NA	$(0.80 \pm 179.3) \times 10^{-1}$	$(0.03 \pm 1.09) \times 10^{2}$

Figure Captions

Figure 1: Structures and abbreviations for the various naphthoic acids used in this work.

Figure 2: (a) Aromatic region of the ^{1}H NMR spectrum of 1NA as a function of concentration. ^{1}H chemical shifts as a function of concentration for (b) 1NA and (c) 2NA. The solid lines are a fit to eq 1.

Figure 3: (a) ^{1}H and (b) ^{19}F spectra of 6F2NA as a function of concentration. ^{1}H chemical shifts for (c) 4F1NA and (e) 6F2NA, ^{19}F chemical shifts for (d) 4F1NA and (f) 6F2NA as a function of concentration. The solid lines are a fit to eq 1.

Figure 4: ^{1}H-measured diffusion coefficients for the four naphthoic acid isomers as a function of sample concentration. Error bars represent the errors in the diffusion coefficient arising from the fitting as calculated by DOSY Toolbox.

Figure 5: ^{1}H chemical shifts for 1NA with (a) 1mol% 4F1NA, (b) 1mol% 6F2NA, and 2NA with (c) 1mol% 4F1NA, (d) 1mol% 6F2NA. The solid lines are a fit to eq 1.

Figure 6: ^{19}F chemical shifts for 1NA with (a) 1mol% 4F1NA, (b) 1mol% 6F2NA, and 2NA with (c) 1mol% 4F1NA, (d) 1mol% 6F2NA. The concentrations given are those of the major naphthoic acid component. The solid lines are a fit to eq 2.

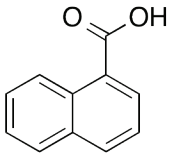

1NA

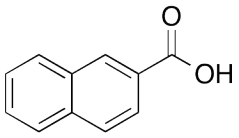

2NA

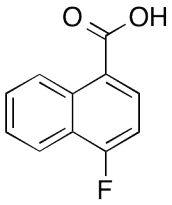

4F1NA

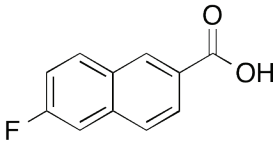

6F2NA

(a)

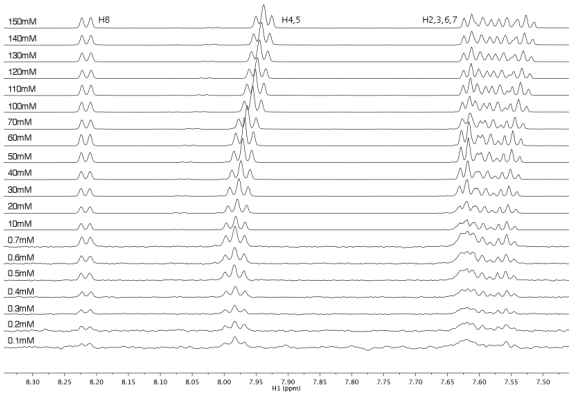
H8
H4,5
H2,3,6,7
150mM
140mM
130mM
120mM
110mM
100mM
70mM
60mM
50mM
40mM
30mM
20mM
10mM
0.7mM
0.6mM
0.5mM
0.4mM
0.3mM
0.2mM
0.1mM
8.30 8.25 8.20 8.15 8.10 8.05 8.00 7.95 7.90 7.85 7.80 7.75 7.70 7.65 7.60 7.55 7.50
H1 (ppm)

(b)

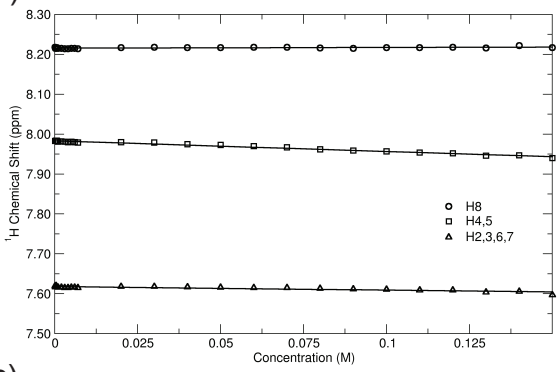
8.30
8.20
8.10
8.00
7.90
7.80
7.70
7.60
7.50
0
0.025
0.05
0.075
0.1
0.125
Concentration (M)
^{1}H Chemical Shift (ppm)
H8
H4,5
H2,3,6,7

(c)

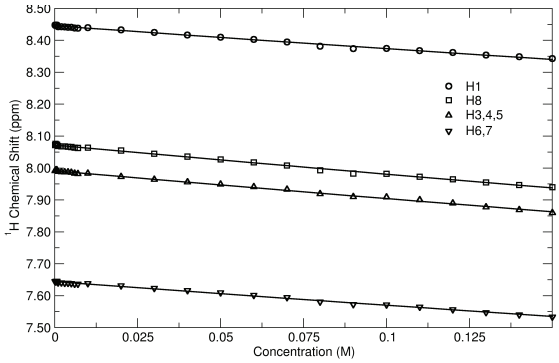
8.50
8.40
8.30
8.20
8.10
8.00
7.90
7.80
7.70
7.60
7.50
0
0.025
0.05
0.075
0.1
0.125
Concentration (M)
^{1}H Chemical Shift (ppm)
H1
H8
H3,4,5
H6,7

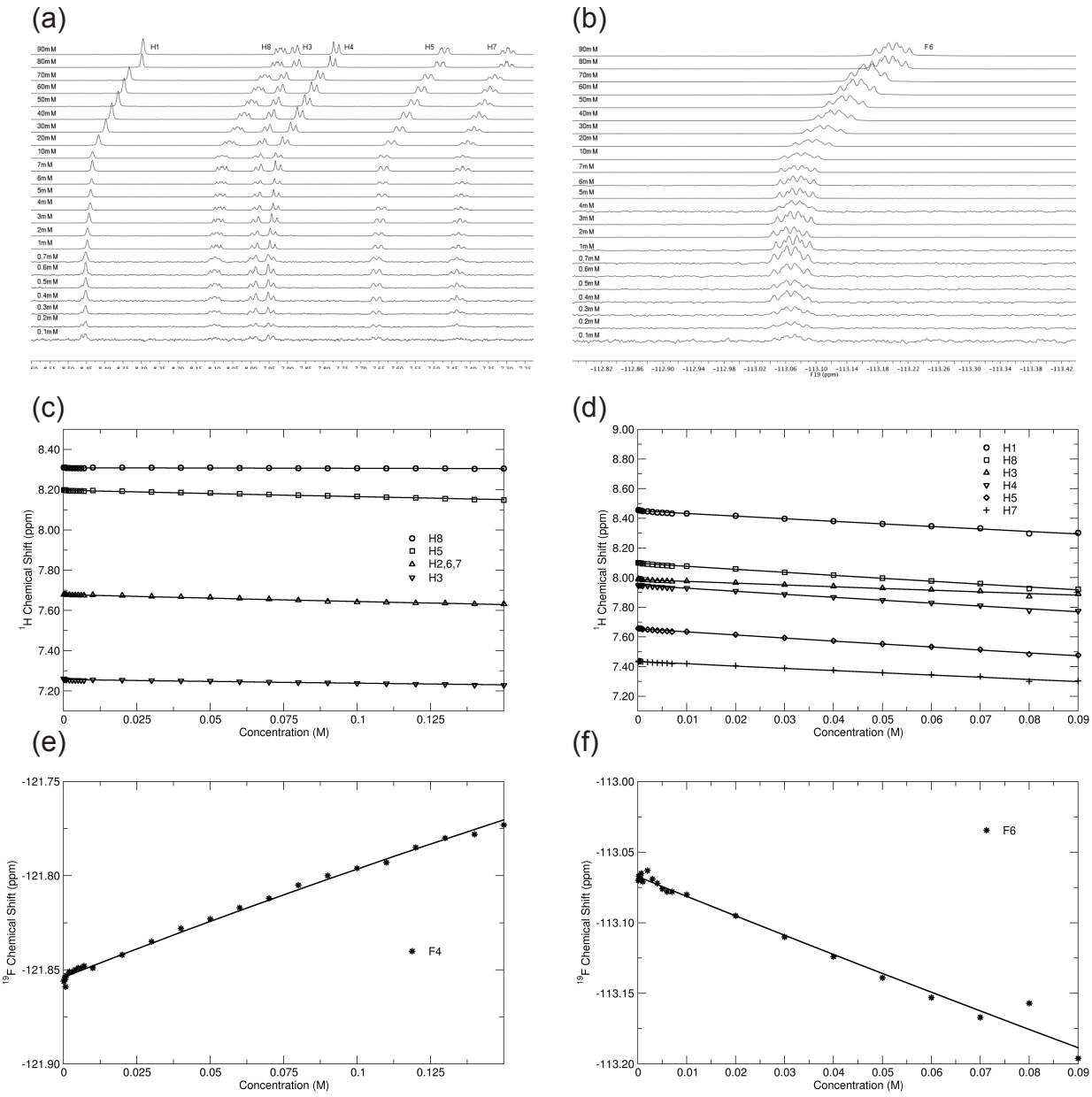
(a)
H1
H8
H3
H4
H5
H7
90m M
80m M
70m M
60m M
50m M
40m M
30m M
20m M
10m M
7m M
6m M
5m M
4m M
3m M
2m M
1m M
0.7m M
0.6m M
0.5m M
0.4m M
0.3m M
0.2m M
0.1m M
(b)
F6
F19 (ppm)
(c)
^{1}H Chemical Shift (ppm)
Concentration (M)
H8
H5
H2,6,7
H3
(d)
^{1}H Chemical Shift (ppm)
Concentration (M)
H1
H8
H3
H4
H5
H7
(e)
^{19}F Chemical Shift (ppm)
Concentration (M)
F4
(f)
^{19}F Chemical Shift (ppm)
Concentration (M)
F6

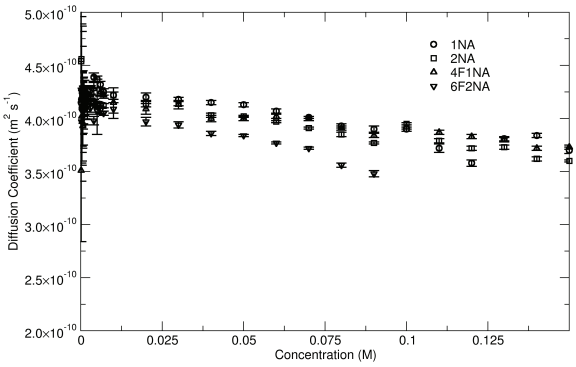
5.0×10^-10
4.5×10^-10
4.0×10^-10
3.5×10^-10
3.0×10^-10
2.5×10^-10
2.0×10^-10
Diffusion Coefficient (m^2 s^-1)
0
0.025
0.05
0.075
0.1
0.125
Concentration (M)
1NA
2NA
4F1NA
6F2NA

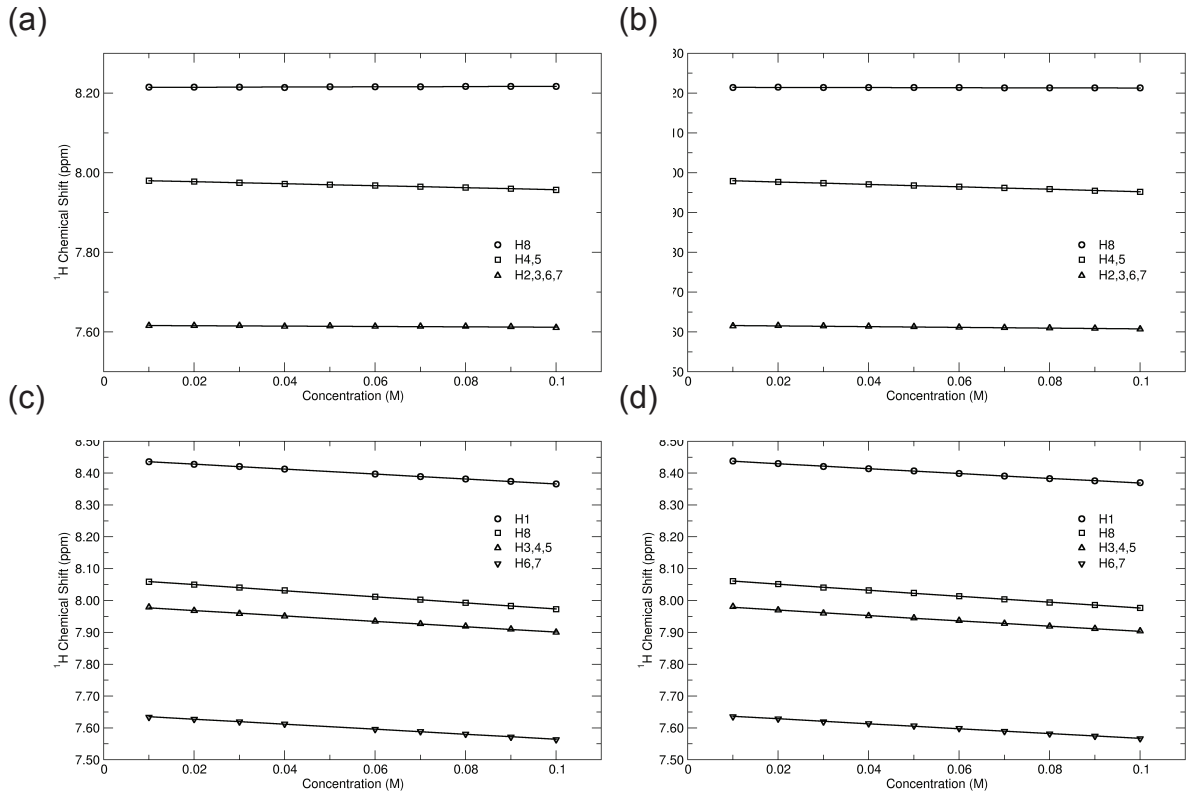
(a)
(b)
(c)
(d)
^{1}H Chemical Shift (ppm)
Concentration (M)
H8
H4,5
H2,3,6,7
H1
H3,4,5
H6,7

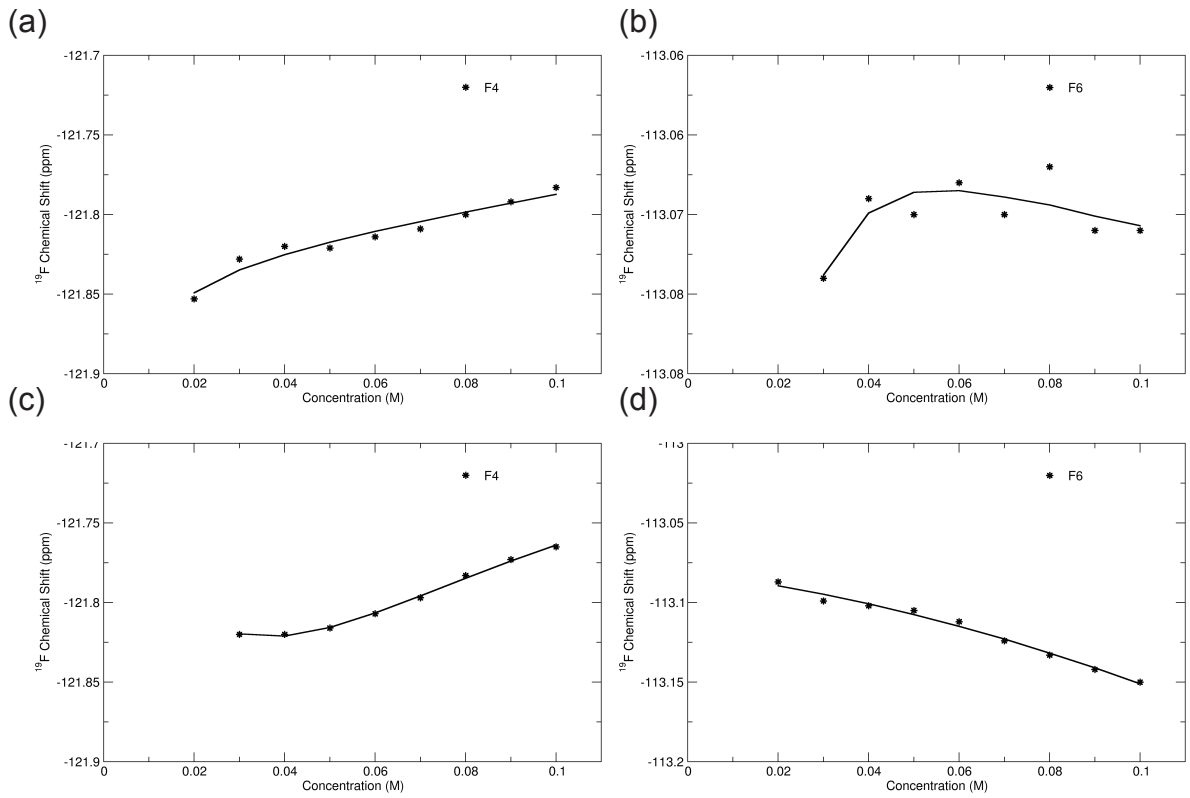
(a)
(b)
(c)
(d)
F4
F6
^{19}F Chemical Shift (ppm)
Concentration (M)
-121.7
-121.75
-121.8
-121.85
-121.9
-113.06
-113.07
-113.08
-113.05
-113.1
-113.15
-113.2
0
0.02
0.04
0.06
0.08
0.1